Proceedings of Meetings on Acoustics

Volume 19, 2013 http://acousticalsociety.org/

ICA 2013 Montreal
Montreal, Canada
2 - 7 June 2013

Underwater Acoustics
Session 2aUW: Wave Propagation in a Random Medium

2aUW2. The effect of surface and linear internal waves on higher order acoustic moments in shallow water

Kaustubha Raghukumar* and John Colosi

***Corresponding author's address: Oceanography, Naval Postgraduate School, 833 Dyer Road, Monterey, CA 93943, kraghuku@nps.edu**

Acoustic fields in shallow water have a statistical nature due to complex, time-evolving sound speed fields and scattering from rough boundaries. Previously, coupled-mode transport theory [Raghukumar and Colosi (2012)] was applied to high frequency acoustic fluctuations in an environment typical of the Shallow Water 2006 (SW06) experiment on the New Jersey continental shelf. As a consequence of the strong adiabatic component in SW06 propagation, a hybrid approach was used to calculate mode coherences where mode energies from the Dozier-Tappert approach were combined with adiabatic phase terms. Mode energies, coherences and acoustic intensities were examined and it was found that internal and surface waves preferentially couple low and high modes respectively. Here, we extend that study to include higher moments such as scintillation index and shift focus to modes that are coupled by both internal and surface waves. Oceanographic and sea surface measurements are used to constrain the internal wave and sea surface models. The relative importance of linear internal waves and surface scattering effects are studied using transport theory and Monte Carlo simulations.

Published by the Acoustical Society of America through the American Institute of Physics

Received 22 Jan 2013; published 2 Jun 2013
Proceedings of Meetings on Acoustics, Vol. 19, 070022 (2013)

INTRODUCTION

The coastal ocean is a shallow water environment that is often subject to intensive internal and surface wave activity, as well as seabed roughness, all of which lead to a statistical nature for shallow water acoustic fields. While random linear internal waves are a dominant cause of acoustic fluctuation at low frequencies (Colosi *et al.*, 2012), surface waves play an important role at higher frequencies due to the greater role played by surface interacting acoustic modes (Thorsos *et al.*, 2004).

The acoustic field in a fluctuating environment can be described by quantities such as the mean and variance of acoustic intensity, and a measure of coherence. While these quantities can be obtained by full-physics Monte Carlo simulations (Headrick *et al.*, 2000), reduced-physics models based on transport theory (Colosi and Morozov, 2009) directly compute the desired metrics in addition to providing physical insight on the acoustically relevant scales of oceanographic fluctuations.

Here we examine the predictability of acoustic fluctuations in shallow water at high frequencies (1500 Hz), and examine the ocean processes that contribute most strongly to acoustic variability. We focus our attention on two key processes important to shallow water acoustics: random linear internal waves as described by a shallow water version of the Garett-Munk spectrum, and random surface gravity waves as described by the Pierson-Moskowitz spectrum. A comprehensive transport theory that accounts for internal wave-induced sound speed perturbations along with rough surface scattering is presented in this work.

Previously, theoretical estimates of the cross mode coherence matrix, mean intensity, and time and depth coherence have showed excellent agreement with Monte Carlo simulations in a variety of deep (Colosi and Morozov, 2009; Colosi *et al.*, 2012, accepted for publication; Chandrayadula *et al.*, 2012, accepted for publication) and shallow water scenarios (Colosi *et al.*, 2012) at low frequency in the presence of linear and non-linear internal waves. Additionally, Thorsos *et al.* (2004, 2010) have developed a transport theory to explain the evolution of mode coherence by surface scattering mechanisms. Transport theory allowed for several physical insights into the mechanism of mode coupling previously lacking in Monte Carlo simulations in addition to a vastly reduced computational effort. In shallow water, Colosi *et al.* (2012) have shown that the acoustic variability seen for nonlinear waves alone is much different from the effects seen for linear and nonlinear internal waves together. Similar behavior is demonstrated here when the treatment of a rough sea surface and linear internal waves are included together.

TRANSPORT THEORY

Using a 2D normal mode-based approach, the acoustic pressure field, $p(r,z)$ can be expressed as

$$p(r,z) = \sum_{n=1}^{N} \frac{a_n(r)\phi_n(z)}{\sqrt{k_n r}} \tag{1}$$

where $\phi_n(z)$ is the unperturbed mode shape, with all variability contained in the range-dependent mode amplitude, $a_n(r)$, and the complex eigen-wavenumber $l_n = k_n + i\alpha_n$.

Creamer (1996) expressed the evolution of mode amplitudes in shallow water as

$$\frac{da_n}{dr} - il_n a_n = -i \sum_{m=1}^{N} \Gamma_{mn}(r) a_m(r) \tag{2}$$

where $\Gamma_{mn}(r)$ is the symmetric coupling matrix, which in the presence of internal wave-induced sound speed perturbations, is given by

$$\Gamma_{mn}(r) = \frac{k_0^2}{\sqrt{k_n k_m}} \int_0^D \frac{\phi_n(z)\phi_m(z)}{\rho_0(z)} \frac{\delta c(r,z)}{c_0} dz \tag{3}$$

where $\delta c(r,z)$ is the sound speed perturbation for a background sound speed c_0, D is the water depth, $\rho_0(z)$ is the density profile and $k_0 = \omega/c_0$ is a representative wavenumber. On the other hand, in the presence of surface waves, the symmetric mode coupling matrix is given by (Thorsos *et al.*, 2004)

$$\Gamma_{mn}(r) = -\frac{h(r)}{2\rho_0(0)} \frac{1}{\sqrt{k_n k_m}} \frac{d\phi_m}{dz} \frac{d\phi_n}{dz} \tag{4}$$

where $h(r)$ is the surface displacement, and the derivatives are evaluated at $z = 0$.

Transport theory provides expressions for the range evolution of various moments of intensity such as the first moment, $\langle I \rangle = \langle |p|^2 \rangle$, and second moment $\langle I^2 \rangle = \langle |p|^4 \rangle$. The mean intensity can be expressed as

$$\langle I(r,z) \rangle = \langle |p(r,z)|^2 \rangle = \sum_{n=1}^{N} \sum_{p=1}^{N} \frac{\langle a_n(r) a_p^*(r) \rangle}{r} \frac{\phi_n(z)\phi_p(z)}{\sqrt{k_n k_p}} \tag{5}$$

where $\langle a_n(r) a_p^*(r) \rangle$ can be recognized as the cross-mode coherence matrix. Dozier and Tappert (1978) proposed a transport theory for the range evolution of mode energies $\langle |a_n|^2 \rangle$, or the diagonal of the cross-mode coherence matrix, in the absence of sub-bottom attenuation. Creamer's transport theory contained expressions for the range evolution of the full cross-mode coherence matrix, although the analysis was confined to the mode energy terms. Colosi and Morozov (2009) provided a more heuristic derivation of Creamers transport theory, and undertook a deeper analysis of the range evolution of the cross-mode coherence terms. Of particular interest was their result that in an environment dominated by mode coupling, both mode energies and cross-mode coherences decay with range at a similar rate. In a more recent paper, Colosi *et al.* (2012) applied transport theory to a shallow water environment typical of the SW06 experiment on the Mid-Atlantic bight (Lynch and Tang, 2008). At frequencies between 200-400 Hz, and over distances of tens of kilometers, a simple adiabatic theory was shown to sufficiently explain most of the propagation physics.

The range evolution of the cross-mode coherence matrix is given by

$$\frac{d\langle a_n a_p^* \rangle}{dr} + i(l_p^* - l_n)\langle a_n a_p^* \rangle = \sum_{m=1}^{N} \sum_{q=1}^{N} \langle a_m a_q^* \rangle I_{mn,qp}^* + \langle a_q a_m^* \rangle I_{mp,qn} - \langle a_n a_q^* \rangle I_{mp,qm}^* - \langle a_q a_p^* \rangle I_{mn,qm} \tag{6}$$

where $I_{mn,qp}$, known as the scattering matrix is given by

$$I_{mn,qp} = \int_0^\infty d\xi \Delta_{mn,qp}(\xi) e^{-ik_{qp}\xi} \tag{7}$$

where $\Delta_{mn,qp}(\xi) = \langle \Gamma_{mn}(r)\Gamma_{qp}(r+\xi) \rangle$ is the correlation function of the symmetric mode coupling matrix for range separation ξ, in the presence of either internal or surface waves (Eqs. 3,4 respectively). The mode wavenumber difference is $k_{qp} = k_p - k_q$.

Following Colosi *et al.* (2012), the scattering matrix for GM internal waves can be analytically derived as

$$I_{mn,qp} = \sum_{j=1}^{J} G_{mn}(j) G_{qp}(j) H(j) \frac{4a}{\pi |k_{qp}|} \left[\frac{\cos\theta_{min}}{(a^2+1)(a^2+2-a^2\cos 2\theta_{min})} + \frac{\operatorname{atanh}\left(\sqrt{\frac{a^2}{a^2+1}}\cos\theta_{min}\right)}{2a(a^2+1)^{3/2}} + i\frac{\pi}{4a(a^2+1)^{3/2}} \right] \tag{8}$$

where J is the maximum internal wave mode number, $\alpha = k_j/|k_{qp}|$, k_j the internal wave wavenumber, $\sin\theta_{min} = |k_{qp}|f/(k_j N_{max})$, with N_{max} the maximum buoyancy frequency and f the inertial frequency, and $H(j) = N_j/(j^2 + j_*^2)$ is the GM vertical mode spectrum with N_j being the normalization. For the special case of $k_{qp} = 0$, the terms following $H(j)$ in Eq. 8 simplify to $\frac{2}{\pi}\frac{1}{k_j}\frac{k_{max}^2}{k_{max}^2+k_j^2}$. Lastly,

$$G_{mn}(j) = k_0^2\sqrt{\frac{2}{k_n k_m}}\int_0^D dz\langle\mu^2(z)\rangle^{1/2}\sin[\pi j\hat{z}(z)]\frac{\phi_n(z)\phi_m(z)}{\rho_0(z)} \tag{9}$$

with $\hat{z}(z)$ being the WKB stretched vertical coordinate (Colosi *et al.*, 2012).

The scattering matrix for surface waves can be written as

$$I_{mn,qp} = \frac{1}{4\rho^2(0)}\frac{d\phi_m}{dz}\frac{d\phi_n}{dz}\frac{d\phi_q}{dz}d\phi_p dz\int_0^\infty \frac{S_h(k)}{\sqrt{k^2 - k_{qp}^2}}dk \tag{10}$$

where $S_h(k)$ is the surface wave horizontal wavenumber spectrum with $k = \sqrt{k_x^2 + k_y^2}$. Following Thorsos *et al.* (2004), the surface waves are modeled using the Pierson-Moskowitz spectrum, given by

$$S_h(k) = \frac{\alpha}{2k^3}\exp\Big(-\frac{k_L^2}{k^2}\Big] \tag{11}$$

where $\alpha = 8.1\times10^{-3}$, $k_L^2 = \beta g/U^4$, $\beta = 0.74$, $g = 9.8\ m/s^2$, and U is the wind speed in m/s.

Because internal and surface waves are uncorrelated, a superposition of the scattering matrices in Eqs. 8 and 10 can be used in the transport equation, Eq. 6, to predict the range evolution of the cross-mode coherence matrix.

Hybrid theory

At high frequencies (>1kHz), the numerical solution of Eq. 6 was found to exhibit strong instabilities. An approximate solution has been sought by first recognizing that the evolution of mode energies is insensitive to the off-diagonal coherence terms (Colosi and Morozov, 2009). As a result, mode energies can be obtained by solving Creamers equation

$$\frac{d|a_n|^2}{dr} = -2\alpha_n\langle|a_n|^2\rangle + \sum_{m=1}^{N} 2Re(I_{mn,mn})\Big(\langle|a_m|^2\rangle - \langle|a_n|^2\rangle\Big). \tag{12}$$

Next, it is recognized that the off-diagonal elements of the cross-mode coherence matrix have a strong adiabatic component. As a result, a hybrid approach is proposed where the adiabatic expression for the evolution of mode coherences (Eq. 28 in Colosi and Morozov (2009)) is adjusted for range evolution of mode amplitudes, to give

$$\langle a_n a_p^*\rangle(r) = \langle|a_n|^2\rangle^{1/2}(r)\langle|a_p|^2\rangle^{1/2}(r)e^{i(\theta_n(0)+\theta_p(0))}e^{i(l_n - l_p^*)r}e^{-(I_{nn,nn}-2I_{nn,pp}+I_{pp,pp})r} \tag{13}$$

where $\theta_n$is the initial phase of the mode (for a point source, θ_n is either 0 or π).

Edge effect

Inherent to the transport theory explained thus far is the assumption that the range r is longer than the correlation length of internal or surface waves. While this assumption is valid at long ranges, it breaks down at short ranges, close to the receiver, and incorrectly predicts mode coherences at these short ranges. As a result, a correction is needed to account for this edge effect, as provided by Colosi *et al.* (2012), Eq. 18. We will not go into details of this correction in the present manuscript.

RESULTS

A combined transport theory that predicts the evolution of the cross-mode coherence matrix in the presence of internal and surface waves is demonstrated here in a shallow water environment. Fig. 1 shows a sound speed profile with a weak surface duct measured during the SW06 experiment, along with a buoyancy profile and a subset of propagating acoustic modes at 1500 Hz. A point source is located at a depth of 25 m, at the sound speed minimum. The range evolution of mode energies and coherences is calculated out to 50 km. Three different

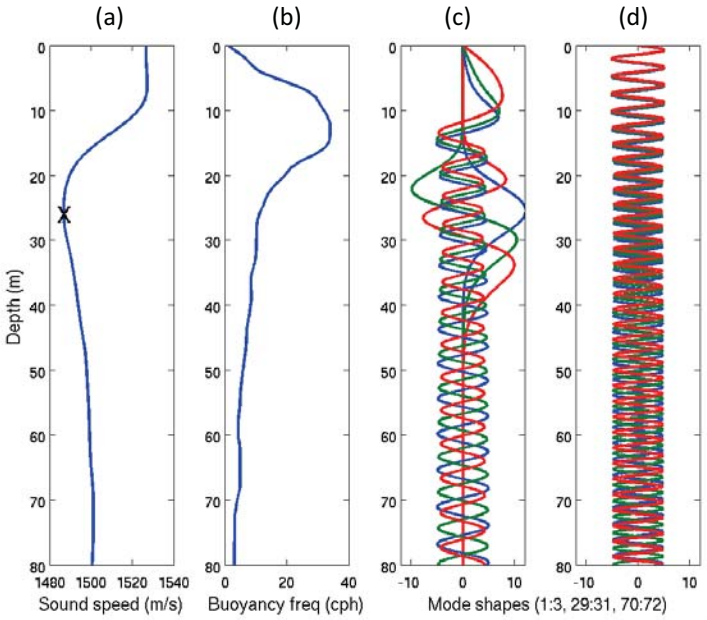

FIGURE 1: (a) SW06 sound speed profile, along with source location, **(b)** Buoyancy frequency, **(c,d)** Acoustic modes, 1-3, 29-31, 71-73

fluctuation scenarios are demonstrated: internal wave scattering, surface wave scattering, combined internal and surface wave scattering.

A metric that shows the degree of mode coupling for the three cases can be obtained by examining Eq. 12. This equation is similar to a diffusion equation, where the matrix $Re(I_{mn,mn})$ facilitates energy transfer from mode m to mode n, and the rate depends on the mode energy difference. Under the small angle forward scattering assumption, mode coupling can be shown to be dominated by nearest neighbor coupling. The first off-diagonal element is a measure of nearest-neighbor mode coupling, and is shown in Fig. 2. Internal waves are predicted to preferentially couple lower order modes, and surface waves preferentially couple higher order modes, increasing with wind speed. Since previous work (Raghukumar and Colosi, 2012) contains results for the lowest- and highest-order modes, at this time results for intermediate modes 29-31 are shown. These modes (Fig. 2) are particularly interesting as they lay on the mode number threshold between internal and surface wave coupling. From Fig. 2, coupling by mode 29 can be expected to be dominated by internal wave scattering, mode 30 by both internal and surface waves, while coupling by mode 30 should be dominantly influenced by surface waves.

Monte Carlo simulations are employed to demonstrate the validity of transport theory, and are shown only for the case with internal wave scattering alone. Mode amplitudes are computed using Eq. 2 for 200 realizations of the internal wave field. Intensity statistics are then computed by appropriately averaging the mode amplitudes. Sub-bottom attenuation is not included at

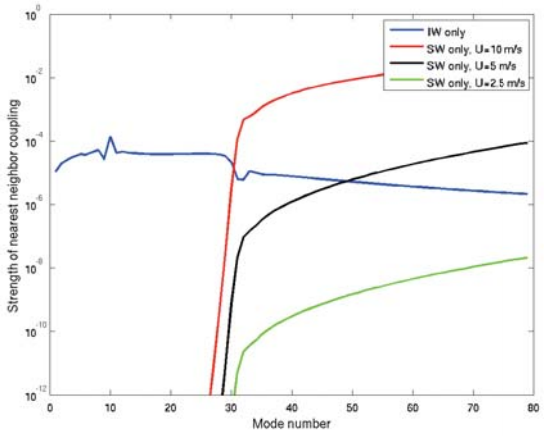

FIGURE 2: Mode coupling metric (m^{-1}) in the presence of internal waves, and surface waves generated by wind speeds of 2.5-10 m/s

present in order to focus exclusively on mode coupling effects.

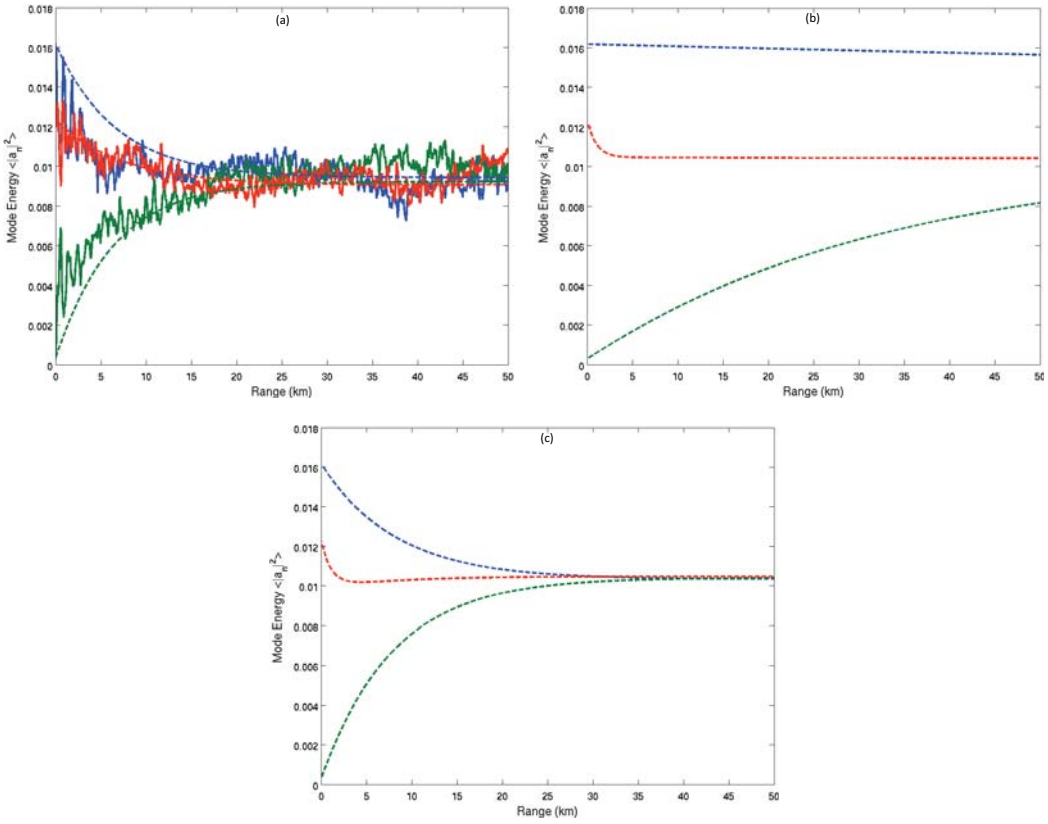

FIGURE 3: Mode energies for modes 29 (Blue), 30 (Green) and 31 (Red). **(a)**: Internal wave scattering, **(b)**: Surface wave scattering, **(c)**: Internal and surface wave scattering. Transport theory is the dotted line, and Monte Carlo simulation is the dashed line.

Fig. 3 shows mode energies for modes 29-31 for the three scattering scenarios. Fig. 3(a), transport theory results (Eq. 12) are overlaid with Monte Carlo simulations for the case with internal wave scattering alone, and the two are seen to be in reasonable agreement. As expected, modes 29,30 show a stronger coupling (slope) by internal waves than mode 31. Next,

Fig. 3(b) shows mode energies as influenced by surface scattering alone. Mode 29 is observed to be unaffected by surface wave-induced mode coupling, and exhibits mostly adiabatic propagation. While mode 30 is somewhat coupled by surface scattering, coupling of this mode is weaker than with internal wave scattering. Finally, mode 31 experiences strong coupling within the first 200 m, and is driven to equal energy with its neighbors soon after. This distance to energy equipartition is closely related to the surface wave correlation length and will be studied in future work. Fig. 3(c) shows the evolution of mode energies as a result of both internal and surface wave scattering. Mode 29 is only affected by internal waves, and mode 31 only by surface waves. Both these modes show behavior identical to the top left and right panels. Mode 30, affected by both internal and surface waves, shows a superposition of both effects.

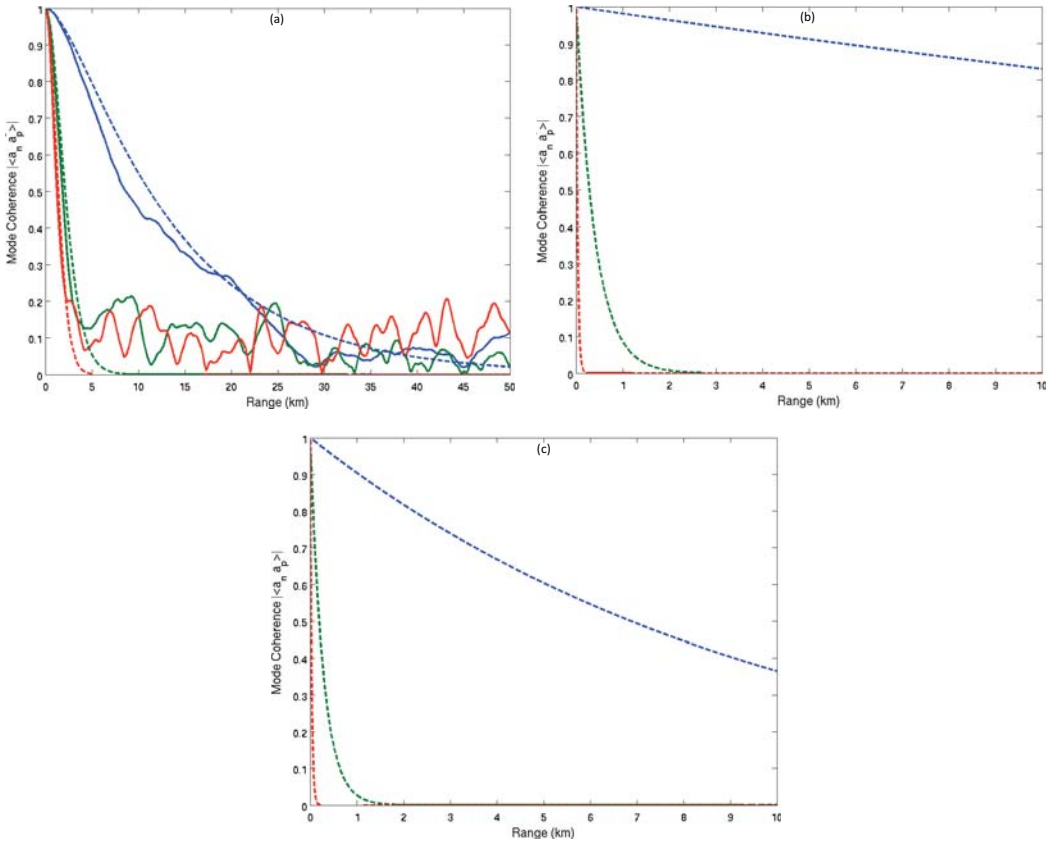

FIGURE 4: Mode coherences of mode 29 with mode 30 (Blue), mode 31 (Green) and mode 32 (Red). **(a)**: Internal wave scattering, **(b)**: Surface wave scattering, **(c)**: Internal and surface wave scattering.Transport theory is the dotted line, and Monte Carlo simulation is the dashed line.

The range evolution of mode coherences of mode 29 with modes 30,31,32 is shown in Fig. 4 for the three scattering scenarios. For the case with internal wave scattering (Fig. 4(a)), good agreement is seen between hybrid transport theory (dashed) and Monte Carlo simulations (dotted). In this case, modes 29 and 30 experience mode coupling, while modes 31 and 32 are not as strongly affected. As a result the phase relationship (coherence) between modes 29-30 is better preserved than with the other two modes. However, with surface wave scattering (Fig. 4(b), note the different range scale), modes 29-30 are now unaffected by surface waves, and preserve an almost perfect coherence across range. Modes 31 and 32 are affected by surface waves in increasing order (Fig. 2), and this is corroborated in the different rates at which their coherence with mode 29 decays. The strong mode coupling of these higher modes results in a rapid phase randomization and loss of coherence. Finally, Fig. 4(c) shows the combined effect of internal and surface waves on mode coherence. The coherences are a combination of effects from

the first two cases. The coherences of modes 29 with 30 is identical to the case with internal wave scattering alone, modes 29 with 31 a superposition of both effects and mode 29 with 32 identical to the case with surface wave scattering alone.

CONCLUSION

Transport theory is an efficient and accurate reduced-physics model that has been used in this paper to provide physical insights into acoustic scattering by internal and surface waves. Mode energies and coherences as treated by hybrid transport theory show good agreement with Monte Carlo simulations. It was previously shown that internal waves preferentially couple lower-order modes while surface waves couple higher-order modes. In this paper, mode energies and coherences of modes that lay on the threshold between internal and surface wave scattering are discussed. Modes that are coupled by both phenomena are shown to have energies and coherences that are almost a linear superposition of the two effects. In other words, while any one effect preserves coherence for a subset of propagating modes, the combined effect results in a loss of coherence across all modes. This is expected to have a significant effect on mean intensity and scintillation index.

ACKNOWLEDGMENTS

This work is supported by the Office of Naval Research. Kaustubha Raghukumar is grateful to the National Academy of Sciences for support through the National Research Council research associateship program.

REFERENCES

Chandrayadula, T., Colosi, J., Dzieciuch, M., Worcester, P., Andrew, R., Mercer, J., and Howe, B. (**2012, accepted for publication**). "Observations and transport theory analysis of low frequency, long range mode propagation in the eastern north pacific ocean", J. Acoustic Soc. Am. .

Colosi, J., Chandrayadula, T., Voronovich, A., and Ostashev, V. (**2012, accepted for publication**). "Coupled mode transport theory for sound transmission through an ocean with random sound speed perturbations: Coherence in deep water environments", J. Acoustic Soc. Am. .

Colosi, J., Duda, T., and Morozov, A. (**2012**). "Statistics of low-frequency normal-mode amplitudes in a ocean with random sound-speed perturbations: First and second moments of intensity in shallow-water environments", J. Acoustic Soc. Am. **131**, 1749–1761.

Colosi, J. and Morozov, A. (**2009**). "Statistics of normal-mode amplitudes in a ocean with random sound-speed perturbations: Cross coherence and mean intensity", J. Acoustic Soc. Am. **126**, 1026–1035.

Creamer, D. B. (**1996**). "Scintillating shallow water waveguides", J. Acoustic Soc. Am. **69**, 2825–2838.

Dozier, L. B. and Tappert, F. D. (**1978**). "Statistics of normal mode amplitudes in a random ocean. I.Theory", J. Acoustic Soc. Am. **63**, 353–365.

Headrick, R. H., Lynch, J. F., Kemp, J. N., Newhall, A. E., von der Heydt, K., Apel, J., Badiey, M., sang Chiu, C., Finette, S., Orr, M., Pasewark, B., Turgot, A., Wolf, S., and Tielbuerger, D.

(**2000**). "Modeling mode arrivals in the 1995 swarm experiment acoustic transmissions", The Journal of the Acoustical Society of America **107**, 221–236, URL http://link.aip.org/link/?JAS/107/221/1.

Lynch, J. and Tang, D. (**2008**). "Overview of shallow water 2006 jasa el special issue papers", The Journal of the Acoustical Society of America **124**, EL63–EL65, URL http://link.aip.org/link/?JAS/124/EL63/1.

Raghukumar, K. and Colosi, J. A. (**2012**). "Transport theory applied to shallow water acoustics: The relative importance of surface scattering and linear internal waves", The Journal of the Acoustical Society of America **132**, 1943–1943, URL http://link.aip.org/link/?JAS/132/1943/4.

Thorsos, E. I., Henyey, F. S., Elam, W. T., Hefner, B. T., Reynolds, S. A., and Yang, J. (**2010**). "Transport theory for shallow water propagation with rough boundaries", AIP Conference Proceedings **1272**, 99–105, URL http://link.aip.org/link/?APC/1272/99/1.

Thorsos, E. I., Henyey, F. S., Elam, W. T., Reynolds, S. A., and Williams, K. L. (**2004**). "Modeling shallow water propagation with scattering from rough boundaries", AIP Conference Proceedings **728**, 132–140, URL http://link.aip.org/link/?APC/728/132/1.